World Journal of Gastroenterology

Submit a Manuscript: https://www.f6publishing.com

World J Gastroenterol 2022 July 21; 28(27): 3488-3502

DOI: 10.3748/wjg.v28.i27.3488

ISSN 1007-9327 (print) ISSN 2219-2840 (online)

ORIGINAL ARTICLE

Retrospective Study

Contrast-enhanced ultrasound Liver Imaging Reporting and Data System: Lights and shadows in hepatocellular carcinoma and cholangiocellular carcinoma diagnosis

Gianpaolo Vidili, Marco Arru, Giuliana Solinas, Diego Francesco Calvisi, Pierluigi Meloni, Assunta Sauchella, Davide Turilli, Claudio Fabio, Antonio Cossu, Giordano Madeddu, Sergio Babudieri, Maria Assunta Zocco, Giovanni Iannetti, Enza Di Lembo, Alessandro Palmerio Delitala, Roberto Manetti

Specialty type: Medicine, research and experimental

Provenance and peer review: Invited article; Externally peer reviewed.

Peer-review model: Single blind

Peer-review report's scientific quality classification

Grade A (Excellent): 0
Grade B (Very good): B
Grade C (Good): C
Grade D (Fair): D, D
Grade E (Poor): 0

P-Reviewer: Cao X, China; Kamimura H, Japan; Lu Q, China; Zhou JH, China

A-Editor: Chen Z, China

Received: December 17, 2021
Peer-review started: December 17, 2021
First decision: January 27, 2022
Revised: February 10, 2022
Accepted: June 16, 2022
Article in press: June 16, 2022
Published online: July 21, 2022

Gianpaolo Vidili, Marco Arru, Diego Francesco Calvisi, Pierluigi Meloni, Assunta Sauchella, Davide Turilli, Claudio Fabio, Antonio Cossu, Giordano Madeddu, Sergio Babudieri, Alessandro Palmerio Delitala, Roberto Manetti, Department of Medical, Surgical and Experimental Sciences, University of Sassari, Sassari 07100, Italy

Giuliana Solinas, Department of Biomedical Sciences, Public Health-Laboratory of Biostatistics, University of Sassari, Sassari 07100, Italy

Maria Assunta Zocco, Department of Internal Medicine and Gastroenterology, Fondazione Policlinico Universitario A. Gemelli IRCCS, Catholic University, Rome 00168, Italy

Giovanni Iannetti, Enza Di Lembo, Ultrasound Unit, Ospedale S. Spirito, Pescara 65123, Italy

Corresponding author: Gianpaolo Vidili, MD, Assistant Professor, Department of Medical, Surgical and Experimental Sciences, University of Sassari, 8 Viale San Pietro, Sassari 07100, Italy. gianpaolovidili@uniss.it

Abstract

BACKGROUND

Contrast-enhanced ultrasound (CEUS) is considered a secondary examination compared to computed tomography (CT) and magnetic resonance imaging (MRI) in the diagnosis of hepatocellular carcinoma (HCC), due to the risk of misdiagnosing intrahepatic cholangiocarcinoma (ICC). The introduction of CEUS Liver Imaging Reporting and Data System (CEUS LI-RADS) might overcome this limitation. Even though data from the literature seems promising, its reliability in real-life context has not been well-established yet.

AIM

To test the accuracy of CEUS LI-RADS for correctly diagnosing HCC and ICC in cirrhosis.

METHODS

CEUS LI-RADS class was retrospectively assigned to 511 nodules identified in 269 patients suffering from liver cirrhosis. The diagnostic standard for all nodules was

either biopsy (102 nodules) or CT/MRI (409 nodules). Common diagnostic accuracy indexes such as sensitivity, specificity, positive predictive value (PPV), and negative predictive value (NPV) were assessed for the following associations: CEUS LR-5 and HCC; CEUS LR-4 and 5 merged class and HCC; CEUS LR-M and ICC; and CEUS LR-3 and malignancy. The frequency of malignant lesions in CEUS LR-3 subgroups with different CEUS patterns was also determined. Inter-rater agreement for CEUS LI-RADS class assignment and for major CEUS pattern identification was evaluated.

RESULTS

CEUS LR-5 predicted HCC with a 67.6% sensitivity, 97.7% specificity, and 99.3% PPV ($P < 0.001$). The merging of LR-4 and 5 offered an improved 93.9% sensitivity in HCC diagnosis with a 94.3% specificity and 98.8% PPV ($P < 0.001$). CEUS LR-M predicted ICC with a 91.3% sensitivity, 96.7% specificity, and 99.6% NPV ($P < 0.001$). CEUS LR-3 predominantly included benign lesions (only 28.8% of malignancies). In this class, the hypo-hypo pattern showed a much higher rate of malignant lesions (73.3%) than the iso-iso pattern (2.6%). Inter-rater agreement between internal raters for CEUS-LR class assignment was almost perfect ($n = 511$, $k = 0.94$, $P < 0.001$), while the agreement among raters from separate centres was substantial ($n = 50$, $k = 0.67$, $P < 0.001$). Agreement was stronger for arterial phase hyperenhancement (internal $k = 0.86$, $P < 2.7 \times 10^{-214}$; external $k = 0.8$, $P < 0.001$) than washout (internal $k = 0.79$, $P < 1.6 \times 10^{-202}$; external $k = 0.71$, $P < 0.001$).

CONCLUSION

CEUS LI-RADS is effective but can be improved by merging LR-4 and 5 to diagnose HCC and by splitting LR-3 into two subgroups to differentiate iso-iso nodules from other patterns.

Key Words: Contrast-enhanced ultrasound Liver Imaging Reporting and Data System; Hepatocellular carcinoma; Intrahepatic cholangiocarcinoma; Cirrhosis; Contrast-enhanced ultrasound; Liver

Core Tip: This is a retrospective study to evaluate the accuracy of contrast-enhanced ultrasound Liver Imaging Reporting and Data System (CEUS LI-RADS) in correctly diagnosing hepatocellular carcinoma (HCC) and intrahepatic cholangiocarcinoma (ICC) in patients with cirrhosis. CEUS LR-5 showed a 97.7% specificity for HCC with a low sensitivity (67.6%), while the CEUS LR-4 and 5 merged class showed a 93.9% sensitivity and 94.3% specificity for HCC. CEUS LR-M predicted ICC with a 91.3% sensitivity and 96.7% specificity. CEUS LR-3 predominantly included benign lesions (28.8% of malignancies) but was heterogeneous as the hypo-hypo pattern showed a higher rate of malignant lesions (73.3%) than the iso-iso pattern (2.6%).

Citation: Vidili G, Arru M, Solinas G, Calvisi DF, Meloni P, Sauchella A, Turilli D, Fabio C, Cossu A, Madeddu G, Babudieri S, Zocco MA, Iannetti G, Di Lembo E, Delitala AP, Manetti R. Contrast-enhanced ultrasound Liver Imaging Reporting and Data System: Lights and shadows in hepatocellular carcinoma and cholangiocellular carcinoma diagnosis. *World J Gastroenterol* 2022; 28(27): 3488-3502
URL: https://www.wjgnet.com/1007-9327/full/v28/i27/3488.htm
DOI: https://dx.doi.org/10.3748/wjg.v28.i27.3488

INTRODUCTION

Liver cirrhosis is a strong risk factor for primitive liver cancer, the seventh most commonly diagnosed malignancy worldwide and the third most common cause of cancer-related death[1]. In this scenario, the most prevalent malignant lesion is hepatocellular carcinoma (HCC), followed by intrahepatic cholangiocarcinoma (ICC); however, other types of cancer are rare. The development of a malignant lesion represents a critical point in the clinical history of chronic liver diseases since it significantly reduces life expectancy, especially in case of late diagnosis. Therefore, regular follow-up is essential for these patients with mandatory ultrasonography every 6 mo for detecting solid focal liver lesions[2-5].

Contrast-enhanced ultrasound (CEUS) is an effective, well-recognized, and safe imaging technique for visualising the onset of new nodules in liver cirrhosis, that adheres to national and international guidelines[2,6,7]. One of the initial limitations of CEUS, reported in 2010, was the possibility of missing ICC cases, since a significant proportion of the ICC nodules that develop in a cirrhotic liver show the

same enhancement pattern as HCC[8]. Since then, subsequent studies have demonstrated that the timing and intensity of washout are different in HCC and ICC. In particular, for the vast majority of ICC nodules (50%-85%), washout starts earlier than 60 *s*, while this is rarely observed in HCC. Furthermore, washout intensity during late phase is clearer in ICC than in HCC[9-14]. These findings led the American College of Radiology to release the CEUS Liver Imaging Reporting and Data System (CEUS LI-RADS), similar to previous releases for computed tomography (CT) and magnetic resonance imaging (MRI). The algorithm was officially approved in June 2016, and the latest update was published in 2017 [15].

CEUS LI-RADS is a standardized system for technique, interpretation, reporting, and data collection on focal liver lesions in patients at high risk for HCC. It encompasses features such as size, conventional ultrasound morphology, contrast enhancement behaviours, and dimensional variations in order to stratify the risk of HCC and to avoid ICC misdiagnosis[16-20]. In particular, CEUS LR-5 is a class specifically designed to include HCC. It encompasses nodules > 1 cm that show arterial phase hyperenhancement (APHE) that is neither rim nor globular, followed by a late (> 60 *s*) mild-degree washout. Other CEUS LI-RADS categories (*e.g.*, CEUS LR-4 and 3) express a very probable and intermediate risk of HCC, while CEUS LR-M has an intermediate/high risk of malignancy without a typical HCC pattern. CEUS LR-M includes lesions of any size that show arterial phase rim enhancement pattern and/or early (before 60 *s*) washout and/or marked washout.

So far, only a few studies have presented actual data from the application of CEUS LI-RADS diagnostic algorithm in cirrhotic patients with suspicious nodules[21-27]. The aim of this study was to test the capability of CEUS LI-RADS in accurately diagnosing focal liver lesions in patients affected by cirrhosis. In particular, we tested the accuracy of CEUS LR-5 and LR-M in correctly diagnosing HCC and ICC, respectively. In addition, we merged classes LR-4 and LR-5 and tested their accuracy in correctly diagnosing HCC as a joint class. Finally, we assessed the rate of malignancy for specific LR-3 class patterns.

MATERIALS AND METHODS

Study design and data collection

The present retrospective study involved patients with cirrhosis associated nodules that were visible using conventional ultrasound, for which it was possible to review the basal appearance and dynamic pattern of the ultrasound contrast agent. Cirrhosis was diagnosed on the basis of clinical data, biochemical parameters, imaging criteria, and elastosonography.

We reviewed all the liver CEUS performed at our centre (Medical Ultrasound Unit, University Hospital, Sassari, Italy) between December 2008 and January 2020. All examinations aimed to characterize a new nodule developed in the context of surveillance programmes for liver cirrhosis. Nodules located in different liver segments were analysed separately with individual boluses of contrast. Within the same segment, only one target nodule was included for analysis based on best visualization criteria.

CT and/or MRI, when typical for HCC or definitely benign (haemangioma, hepatic fat deposition/sparing, and hypertrophic pseudomass), were used as the gold standard imaging modalities. For all other cases, histology obtained by a percutaneous biopsy or surgical resection was considered the reference standard (Supplementary Figures 1 and 2).

Specifically, nodules showing a CT/MRI dynamic pattern with hyperenhancement during the arterial phase followed by washout in the portal or late phase (Supplementary Figures 3 and 4), were diagnosed as HCC in accordance with both the American Association for the Study of Liver Diseases (AASLD) and the Italian Association for the Study of the Liver (AISF) guidelines[2,28]. Benign lesions received a further 2-year follow-up; in case of any increase in size and/or CEUS enhancement variations, a biopsy was performed.

All cases where it was not possible to review the timing and the degree of washout on CEUS (23 cases), or a validated diagnostic reference standard, either CT/MRI scan or histology, was not available (35 cases), were excluded. The algorithm of the study is shown in Figure 1.

CEUS examination and CEUS LI-RADS classification

All CEUS examinations were performed by a physician with 15 years of experience (G.V.) using a second-generation ultrasound contrast agent (SonoVue, Bracco, Milan, Italy).

The signal coming from the bubbles was detected through the following ultrasound scanners: (1) Acuson Sequoia 512 with a 4C1 convex probe and cadence contrast pulse sequencing (CPS, Acuson Siemens, Mountain View, CA, United States) until 2014; and (2) Aixplorer (SuperSonic Imaging, S.A., Aix en Provence, France) with a convex broadband probe (SC6-1) and dedicated software also known as Power Modulated Pulse Inversion (PMPI) from January 2015 until the end of the study.

The CEUS examination was performed continuously for 120 s starting from the injection of contrast. Subsequently, short clips lasting 15-30 *s* were recorded until 5 min after injection.

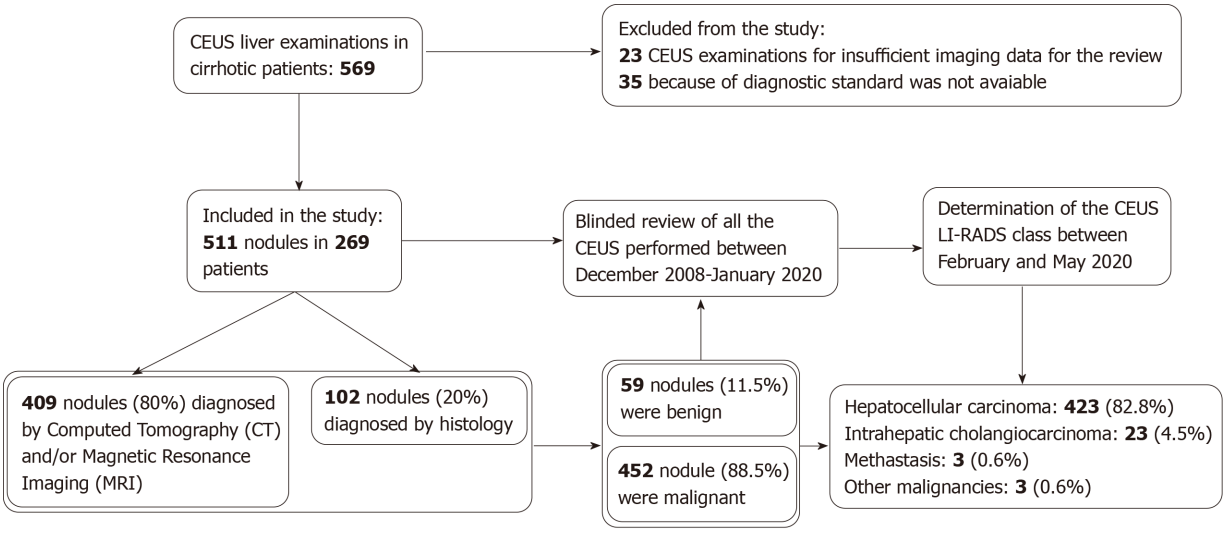

DOI: 10.3748/wjg.v28.i27.3488

Figure 1 Flow chart of the study.

The CEUS LI-RADS patterns were established after evaluation of all clips and images, with particular attention to the behaviour of intranodular contrast enhancement in dynamic phases.

The review process was independently performed by two operators (G.V. and M.A.) with 15 and 2 years of experience, respectively. In case of disagreement, the class indicated by the more experienced operator was assigned.

The reviewers were blinded to patient identity and final diagnosis. The specific targets of the review process were: (1) Nodule size; (2) the presence of APHE and the type of filling (global, rim, or peripheral discontinuous globular enhancement); and (3) the presence of washout during portal and parenchymal phases, focusing on its timing (before or after 60 *s*) and intensity (mild or marked); washout before 60 *s* was considered early, while washout happening after 60 *s* was considered late.

Inter-rater reliability of CEUS LI-RADS class assignment and of CEUS major features between the two raters (internal agreement) was evaluated for all the nodules (n = 511). Inter-rater reliability among our centre and two other operators from external centres (M.A.Z and G.I., both with more than 20 years of experience in CEUS) was also evaluated for a subgroup of 50 nodules (external agreement). To avoid an excess of typical HCCs, a total of 26 HCCs, 11 ICCs, 11 benign lesions, and 2 other malignancies were randomly selected for the external agreement analysis.

The entire process, including folder preparation, CEUS LI-RADS class assignment, and dataset preparation for analysis, was completed over a period of 5 mo. A systematic review of all CT and MRI scans was not performed.

Statistical analysis

Descriptive statistics (median, interquartile range, range, and percentage) were calculated for patients' demographic and clinical characteristics (age, sex, aetiology of cirrhosis, number, and size of nodules). The normal distribution of continuous variables was evaluated through Shapiro-Wilk test. Discrete and qualitative variables are expressed as frequencies and percentages.

Sensitivity, specificity, positive predictive value (PPV), negative predictive value (NPV), diagnostic accuracy, Youden's index, relative risk, odds ratio, positive likelihood ratio, and negative likelihood ratio were calculated to assess the accuracy of different CEUS-LR classes and subclasses in diagnosing HCC (LR-5, LR-4, and LR-4 and 5 merging class), ICC (LR-M), and malignancies (LR-3). The associations between different CEUS LI-RADS classes and definite diagnosis were evaluated by Pearson's chi-square test or Fisher's exact test. To determine the uncertainty of the estimates on sensitivity, specificity, PPV, NPV, and diagnostic accuracy, 95% confidence intervals (CIs) were calculated.

Cohen's k and Fleiss' k statistics were used to evaluate the interobserver agreement among different examiners in the assignment of the CEUS LI-RADS classes and identification of APHE (absent, homogeneous, or rim-like), and washout (absent, late and mild, or early and/or marked). Additionally, a visual graphical representation of the agreement was created, based on the agreement chart proposed by Bangdiwala[29]. All statistical tests were considered significant for a P value < 0.05. Data were analysed using Stata/MP version 17.0 (Statacorp LP, TX, United States) and R version 4.1.1 (The R Foundation for Statistical Computing, Vienna, Austria).

RESULTS

A total of 511 nodules identified in 269 patients were considered in this study. The complete dataset concerning patients and nodule characteristics is shown in Table 1.

Four-hundred and fifty-two out of 511 nodules (88.5%) turned out to be malignant, consisting of 423 HCCs (82.8%), 23 ICCs (4.5%), 3 metastases (0.6%), and 3 other malignancies (0.6%). Non-invasive diagnosis was obtained for 409 nodules (80%), while histology was followed for 102 nodules (20%). Complete data concerning each definite diagnosis rate for every CEUS LI-RADS class are reported in Table 2. Table 3 shows the rates of HCC and ICC in different CEUS LI-RADS classes. The pathological findings for hepatic nodules are shown in Supplementary Table 1.

The most prevalent pattern in the arterial phase was homogeneous APHE (79.1% of all nodules), followed by isoenhancement (12.7%). In the portal and late phases, the majority of nodules showed a late and mild washout (60.7%) while the second most frequent pattern was isoenhancement (30.7%). See Table 4 and Table 5 for complete data on CEUS pattern in the arterial and venous phases, respectively.

LR-M nodules

Thirty-seven lesions (7.2%) were assigned to the CEUS LR-M class (Figure 2A). Twenty-one of these nodules turned out to be ICCs, eleven were HCCs, three were metastases, one was a lymphoepithelioma, and one was benign. CEUS LR-M predicted ICC with a 91.3% sensitivity, 96.7% specificity, 56.8% PPV, 99.6% NPV, and 96.5% diagnostic accuracy ($P < 0.001$) (Table 6). Examining the CEUS behaviour of ICC, it was observed that 16 out of 21 nodules (76%) showed a rim APHE, while 11 out of 21 nodules (52%) showed an early washout (Supplementary Table 2). HCC nodules reported as LR-M showed a rim APHE in 6 out of 11 cases (54.5%) and an early washout in 7 out of 11 cases (63.6%; Supplementary Table 3).

LR-5 nodules

A total of 288 nodules (56.4%) were categorized as CEUS LR-5 (Figure 2B), of which 286 turned out to be HCC, and 2 were benign lesions. The median diameter of these nodules was 25 mm. The conclusive diagnosis was achieved by CT/MRI for 248 nodules and by histology for 40. CEUS LR-5 class predicted HCC with a 67.6% sensitivity, 97.7% specificity, 99.3% PPV, 38.6% NPV, and 72.8% diagnostic accuracy ($P < 0.001$) (Table 6).

LR-4 nodules

One-hundred and fourteen nodules (22.3%) were reported as CEUS LR-4 (Figure 2C), of which 111 were HCC and 3 were regenerative nodules, as confirmed by histology. The median diameter of these nodules was 21.5 mm. In 95 cases, the diagnosis was given by CT/MRI and in 19 cases by biopsy. CEUS LR-4 predicted HCC with a 26.2% sensitivity, 96.6% specificity, 97.4% PPV, 21.4% NPV, and 38.4% diagnostic accuracy ($P < 0.001$) (Table 6). Table 7 show data relative to different LR-4 patterns.

LR 4-5 merged class

The merging of CEUS LR-4 and CEUS LR-5 classes predicted HCC with a 93.9% sensitivity, 94.3% specificity, 98.8% PPV, 76.1% NPV, and 93.9% diagnostic accuracy ($P < 0.001$) (Table 6).

LR-3 nodules

Sixty-six lesions (12.9%) were assigned to the CEUS LR-3 class (Figure 2D and E). Specifically, 15 of these nodules were HCCs, 2 were ICCs, 2 were other malignancies, and 47 were benign lesions. The median diameter of these nodules was 16 mm. Fifty-three lesions were diagnosed non-invasively by CT/MRI, while 13 by biopsy. CEUS LR-3 predicted benign lesions with a 79.7% sensitivity, 95.8% specificity, 71.2% PPV, 97.3% NPV, and 93.9% diagnostic accuracy ($P < 0.001$) (Table 6). Lesions belonging to the CEUS LR-3 class showed great heterogeneity. In fact, iso-iso nodules (Figure 2D) were most likely benign (only 1 malignancy out of 39 nodules), while other patterns showed a higher risk of cancer (18 malignancies out of 27). The second most frequent CEUS LR-3 pattern was the hypo-hypo pattern assigned to 15 nodules (Figure 2E), of which 11 were malignant (7 HCCs, 2 ICCs, 1 lymphoma, and 1 carcinosarcoma). The rate of malignancy for the CEUS LR-3 class and its subclasses are shown in Figure 3. We also calculated the correlation between specific CEUS LR-3 subgroups and malignancy, with analysis limited to CEUS LR-3 nodules ($n = 66$). It was observed that CEUS LR-3 iso-iso pattern predicted malignancy with a 5.3% sensitivity, 19.1% specificity, 2.6% PPV, 33.3% NPV, and 15.2% diagnostic accuracy ($P < 0.001$). Conversely, CEUS LR-3 hypo-hypo pattern predicted malignancy with a 57.9% sensitivity, 91.5% specificity, 73.3% PPV, 84.3% NPV, and 81.8% diagnostic accuracy ($P < 0.001$) (Table 6). Data concerning different LR-3 patterns are reported in Table 7.

LR 1-2 nodules

Only one nodule (0.2%) was categorized as CEUS LR-1, and five nodules (1%) as CEUS LR-2. All these nodules were found to be benign.

Table 1 Characteristics of patients and hepatic nodules

Item	Number or range
Nodules, *n*	511
Patients, *n*	269
Males, *n* (%)	219 (81.4)
Females, *n* (%)	50 (18.6)
Median age at first nodule (IQR; range)	69 years (61-75; 43-88)
Males (IQR; range)	67 years (59-74; 43-88)
Females (IQR; range)	74.5 years (71-78; 59-85)
Hepatic cirrhosis aetiology (n)	
Chronic HCV infection, *n* (%)	129 (48)
Alcohol abuse, *n* (%)	45 (16.7)
Chronic HBV infection, *n* (%)	24 (8.9)
Chronic HCV infection + alcohol abuse, *n* (%)	21 (7.8)
Chronic HBV + HCV infection, *n* (%)	8 (3)
NASH, *n* (%)	6 (2.2)
ChronicHBV infection + alcohol abuse, *n* (%)	5 (1.9)
Other aetiologies, *n* (%)	6 (2.2)
Unknown aetiology, *n* (%)	25 (9.3)
Median diameter of nodules (IQR; range)	24 mm (16-36; 5-200)

IQR: Inter quartile range; HCV: Hepatitis C virus; HBV: Hepatitis B virus; NASH: Non-alcoholic steatohepatitis.

Table 2 Rates of different conclusive diagnoses for each Contrast-enhanced ultrasound Liver Imaging Reporting and Data System class

		Conclusive diagnosis						%
		HCC	ICC	Metastasis	Other malignancy	Benign lesion	Total	
CEUS LI-RADS class	CEUS LR-M	11	21	3	1	1	37	7.2
	CEUS LR-5	286	0	0	0	2	288	56.4
	CEUS LR-4	111	0	0	0	3	114	22.3
	CEUS LR-3	15	2	0	2	47	66	12.9
	CEUS LR-2	0	0	0	0	5	5	1.0
	CEUS LR-1	0	0	0	0	1	1	0.2
	Total	423	23	3	3	59	511	100.0
%		82.8	4.5	0.6	0.6	11.5	100.0	

CEUS LI-RADS: Contrast-enhanced ultrasound Liver Imaging Reporting and Data System; HCC: Hepatocellular carcinoma; ICC: Intrahepatic cholangiocarcinoma.

Interobserver agreement

The observed agreement between the two internal raters (1 and 2) for the assignment of CEUS LI-RADS class was 95.7%, with Cohen's $k = 0.94$ (95%CI: 0.92-0.97, $P < 0.0001$), which represents an almost perfect agreement, according to Landis and Koch[30] classification. The agreement is clearly visualized in Figure 4A. Supplementary Table 4 shows the assignments of the two raters.

The observed agreement among the three raters from different centres (2, 3, and 4) for the assignment of CEUS LI-RADS class was 68% and Fleiss's k coefficient showed a value of 0.67 ($P < 0.0001$), which represents a substantial agreement. In particular, the agreement was almost perfect between raters 2 and

Table 3 Rates of hepatocellular carcinoma and intrahepatic cholangiocarcinoma in different Contrast-enhanced ultrasound Liver Imaging Reporting and Data System classes

CEUS LI-RADS class	HCC	ICC
LR-3	15/66 (22.7%)	2/66 (3%)
LR-4	111/114 (97.4%)	0/114 (0%)
LR-5	286/288 (99.3%)	0/288 (0%)
LR-M	11/37 (29.7%)	21/37 (56.8%)

CEUS LI-RADS: Contrast-enhanced ultrasound Liver Imaging Reporting and Data System; HCC: Hepatocellular carcinoma; ICC: Intrahepatic cholangiocarcinoma.

Table 4 Rates of different contrast-enhanced ultrasound patterns in arterial phase

Arterial phase CEUS pattern	Nodules, *n* (%)
Homogeneous hyperenhancement	404 (79.1)
Rim hyperenhancement	23 (4.5)
Globular hyperenhancement	1 (0.2)
Isoenhancement	65 (12.7)
Hypoenhancement	18 (3.5)

CEUS: Contrast-enhanced ultrasound.

Table 5 Rate of different portal and late phase contrast-enhanced ultrasound patterns

Portal and late phase CEUS pattern	Nodules, *n* (%)
Late and mild washout	310 (60.7%)
Early/marked washout	27 (5.3%)
Isoenhancement	157 (30.7%)
Hypoenhancement	15 (2.9%)
Hyperenhancement	2 (0.4%)

CEUS: Contrast-enhanced ultrasound.

3 (k = 0.88, $P < 1.7 \times 10^{-68}$), substantial between raters 2 and 4 (k = 0.66, $P < 1.5 \times 10^{-14}$), and substantial between raters 3 and 4 (k = 0.61, $P < 8.5 \times 10^{-10}$). The agreement is visualized in Figure 4B-D.

With regards to specific CEUS patterns, we found a higher degree of agreement for APHE (internal k = 0.86, $P < 2.7 \times 10^{-214}$; external k = 0.8, $P < 0.001$) than for washout (internal k = 0.79, $P < 1.6 \times 10^{-202}$; external k = 0.71, $P < 0.001$).

DISCUSSION

CEUS LI-RADS is a valuable diagnostic tool for non-invasive differential diagnosis of focal liver lesions in patients with cirrhosis. Based on our experience, employing this approach improves the performance of CEUS in the characterization of nodules, especially to discriminate between HCC and ICC.

In the current study, CEUS LR-5 was extremely specific for HCC with a very high PPV (99.3%). Only two false-positive results were observed, which were not ICC. We can therefore maintain that CEUS LR-5 is an appropriate tool for non-invasive diagnosis of HCC with virtually no risk of ICC misdiagnosis. Our data agree with recent publications on the subject[22]. However, CEUS LR-5 lacked sensitivity (67.6%) due to the large number of CEUS LR-4 nodules with a final diagnosis of HCC (97.4%). The high specificity of CEUS LR-5 for HCC combined with a low sensitivity was confirmed by a recent prospective multicentric study that compared the accuracy of different CEUS algorithms for the non-

Table 6 Diagnostic statistics of different contrast-enhanced ultrasound Liver Imaging Reporting and Data System classes for different diagnosis

Tested association	Sensitivity (%)	Specificity (%)	PPV (%)	NPV (%)	Diagnostic accuracy (%)	Youden's index	Odds Ratio	*P* value
CEUS LR M-ICC	91.3 (72.0-98.9)	96.7 (94.7-98.1)	56.8 (39.5-72.9)	99.6 (98.5-99.9)	96.5 (94.5-97.9)	0.880	309.75	< 0.001
CEUS LR 5-HCC	67.6 (62.9-72.1)	97.7 (92.0-99.7)	99.3 (97.5-99.9)	38.6 (32.1-45.3)	72.8 (68.7-76.6)	0.653	89.80	< 0.001
CEUS LR 4-HCC	26.2 (22.1-30.7)	96.6 (90.4-99.3)	97.4 (92.5-99.5)	21.4 (17.5-25.8)	38.4 (34.1-42.7)	0.228	10.10	< 0.001
CEUS LR 4/5-HCC	93.9 (91.1-95.9)	94.3 (87.2-98.1)	98.8 (97.1-99.6)	76.1 (67.0-83.8)	93.9 (91.5-95.8)	0.882	253.50	< 0.001
CEUS LR 3-benign lesion	79.7 (67.2-89.0)	95.8 (93.5-97.5)	71.2 (58.7-81.7)	97.3 (95.3-98.6)	93.9 (91.5-95.8)	0.755	89.26	< 0.001
CEUS LR-3-malignancy	4.2 (2.5-6.5)	20.3 (11.0-32.8)	28.8 (18.3-41.3)	2.7 (1.4-4.7)	6.0 (4.2-8.5)	-0.755	0.01	< 0.001
CEUS LR-3-iso-iso-malignancy	5.3 (0.1-26.0)	19.1 (9.1-33.3)	2.6 (0.1-13.5)	33.3 (16.5-54.0)	15.2 (7.5-26.1)	-0.756	0.01	< 0.001
CEUS LR-3-hypo-hypo-malignancy	57.9 (33.5-79.7)	91.5 (79.6-97.6)	73.3 (44.9-92.2)	84.3 (71.4-93.0)	81.8 (70.4-90.2)	0.494	14.78	< 0.001

CEUS: Contrast-enhanced ultrasound; HCC: Hepatocellular carcinoma; ICC: Intrahepatic cholangiocarcinoma; PPV: Positive predictive value; NPV: Negative predictive value.

Table 7 Classification of nodules for LR-3, LR-4, and LR-5 classes, reported in yellow, orange, and red, respectively

Nodule size	No APHE[1]		APHE[1]		Total
	< 20 mm	≥ 20 mm	< 10 mm	≥ 10 mm	
No washout of any type	37 (4)	21 (5)	1 (1)	106 (104)	165
Late and mild washout	7 (5)	8 (7)	0	288 (286)	303
Total	44	29	1	394	468

[1]With the exclusion of nodules with rim and peripheral discontinuous globular arterial phase hyper-enhancement belonging to contrast-enhanced ultrasound LR-M and contrast-enhanced ultrasound LR-1 classes, respectively.
Number of hepatocellular carcinomas in brackets. APHE: Arterial phase hyperenhancement.

invasive diagnosis of HCC[31] and a recent meta-analysis[32].

Considering the high risk of HCC for the LR-4 class (97.4% PPV), the possibility of merging LR-4 and 5 classes was tested. By doing so, sensitivity in identifying HCC rose from 67.6% to 93.9%. The loss in specificity was low (from 97.7% to 94.3%), and was entirely attributed to two nodules > 10 mm classified as CEUS LR-4, which turned out to be benign. Data from the literature supports such an approach, showing that around 50% of HCCs do not display any washout in the portal and late venous phases on CEUS. In particular, Giorgio *et al*[33] demonstrated in their series that 55.4% of the biopsied HCC nodules < 20 mm showed this pattern after APHE. These findings were further corroborated by Leoni *et al*[34], who found that the hyper-iso pattern shows a high PPV (94%) for HCC and identifies nodules that are HCC or with a strong tendency to malignant progression. This pattern was detected in 36.2% (46 out 127) of HCCs[34].

Therefore, it should be considered that the introduction of the washout criteria in CEUS is based on findings from studies exploring the role of contrast-enhanced CT in the non-invasive diagnosis of HCC [35-37]. These findings were then extended to CEUS and MRI with little consideration for the differences in the pharmacokinetics of contrast agents among these techniques and the importance of the nodule visibility at baseline. Indeed, the requirement for washout as a diagnostic criterion is less stringent for CEUS and MRI, since these techniques have an improved capability to evaluate and determine whether APHE reflects the presence of a distinct nodule or merely abnormalities of intrahepatic vessels. CEUS, in particular, is performed for improved characterization of a nodule that has already been detected through conventional ultrasound.

Unfortunately, the introduction of washout in CEUS has significantly lowered the sensitivity of non-invasive diagnostic criteria for HCC. The inclusion of hyper-iso pattern among criteria for non-invasive HCC diagnosis might be a solution to increase CEUS sensitivity. Using this strategy, it can be concluded that there is no significant risk of overestimating the diagnosis of HCC, as in our series 98% of the

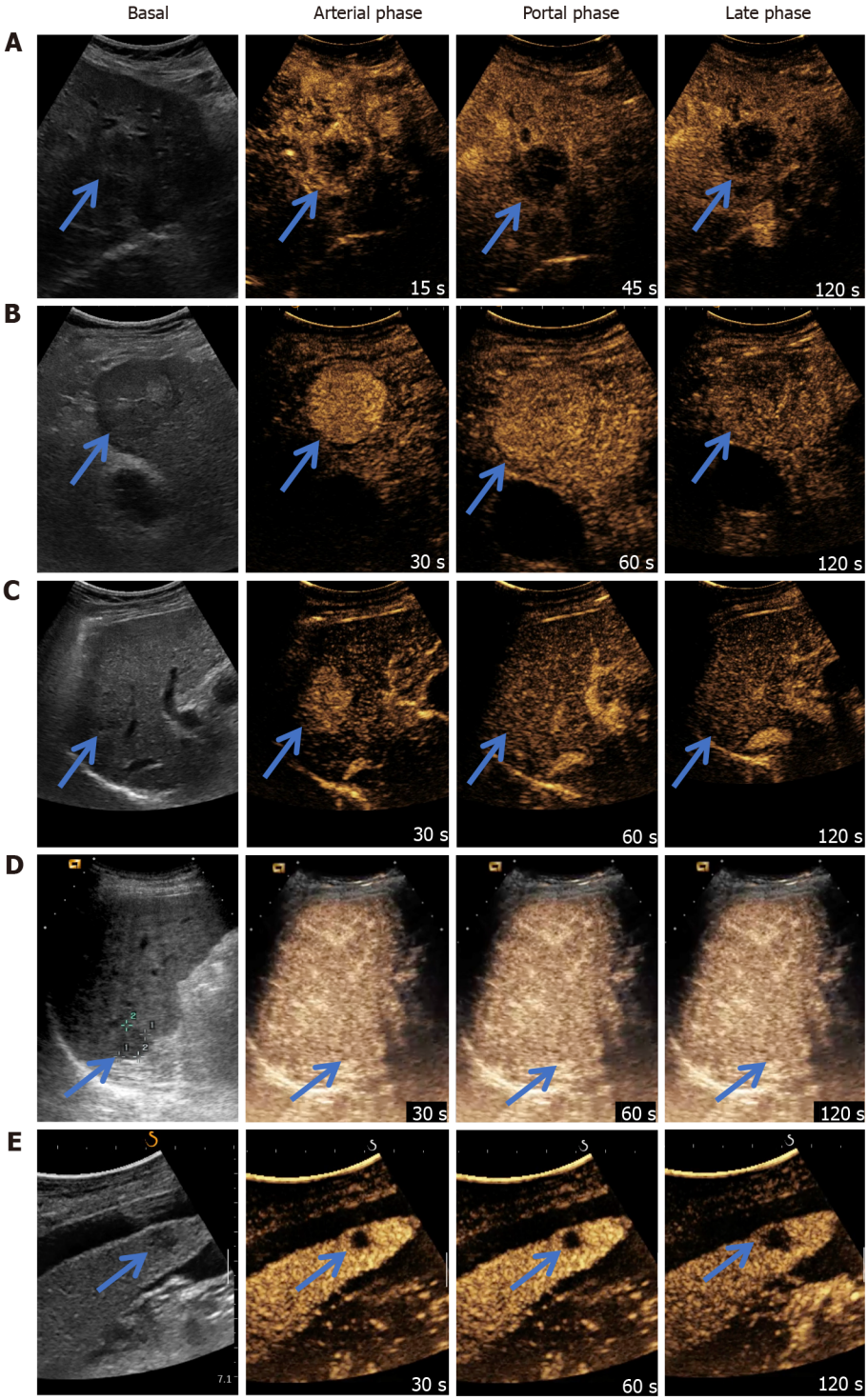

DOI: 10.3748/wjg.v28.i27.3488

Figure 2 Examples of different contrast-enhanced ultrasound Liver Imaging Reporting and Data System classes. A: Contrast-enhanced ultrasound (CEUS) LR-M. Notice rim arterial phase hyperenhancement and early washout, before 60 *s*; B: CEUS LR-5. Notice homogeneous arterial phase hyperenhancement, isoenhancement in portal phase, and mild washout in the late phase; C: CEUS LR-4. Notice homogeneous arterial phase hyperenhancement and isoenhancement in both portal and late phases; D: CEUS LR-3 iso-iso. Notice isoenhancement in all phases; E: CEUS LR-3 hypo-hypo. Notice hypoenhancement in all phases. The arrows show the target lesion.

nodules with the hyper-iso pattern were HCCs and only 2% were benign nodules. These considerations and results agree with another study on the combination of CEUS LR-4 and LR-5 criteria[38]. Furthermore, different studies demonstrated that the identification of washout has higher inter-rater variability than APHE identification[39,40]. These findings are also confirmed by the present study.

Regarding ICC, we observed that the majority of the nodules (21/23, 91.3%) were correctly diagnosed using the LR-M class of risk. Only two ICC cases were not assigned to this class due to a hypovascular aspect in all phases. The high sensitivity and specificity of the CEUS LR-M class for ICC (91.3% and

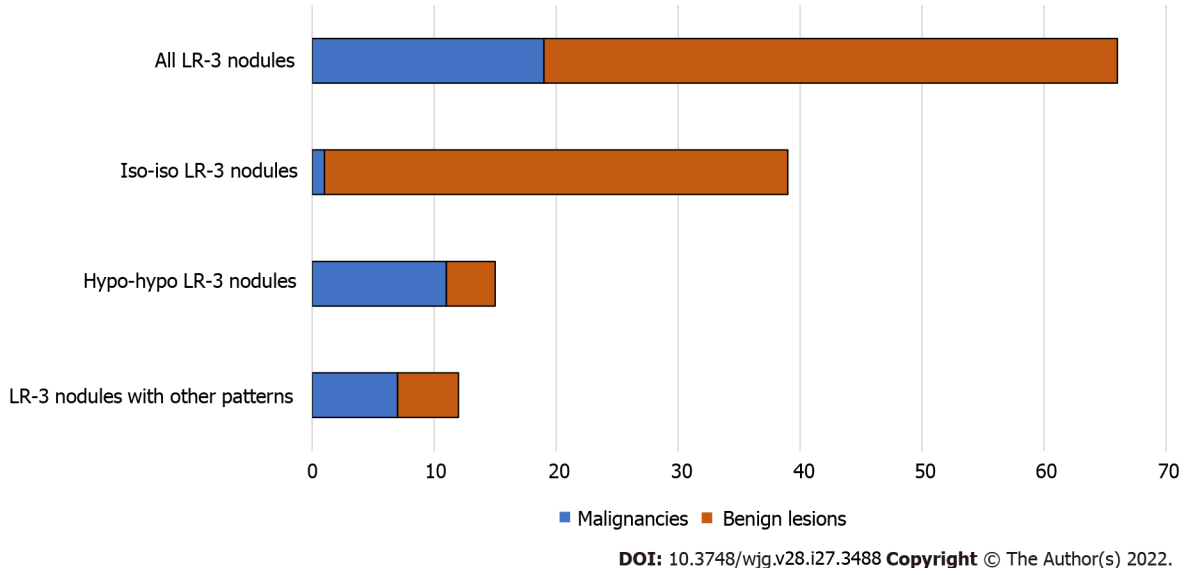

DOI: 10.3748/wjg.v28.i27.3488

Figure 3 Absolute frequency (*n*) of malignancies and benign lesions in LR-3 nodules and LR-3 subgroups with different contrast-enhanced ultrasound patterns.

96.7%, respectively) in our series of patients demonstrate that this class is a valuable diagnostic tool for this type of cancer. Still, this class is not entirely specific for ICC as other types of malignancy can be found, such as HCC, metastatic lesions, and rarer malignancies[41]. We found that 11 out of 37 nodules (30%) classified as LR–M turned out to be HCC. This was due to the presence of an early washout (63.6% of nodules) and/or a rim enhancement pattern (54.5% of nodules). These observations are in agreement with the previously published literature. In particular, a multicentre retrospective study published by Terzi *et al*[22] reported that about 40% of LR-M lesions were HCCs. Another study by Wilson *et al*[16] identified that 35% of HCCs were reported to be LR-M. Several other authors have attempted to decrease the risk of HCC misdiagnosis by proposing a modified LR-M class of risk with the introduction of new criteria, such as the shortening of washout timing to < 45 *s* or the possibility to detect a significant washout to < 3 min[42-44]. Interestingly, Chen *et al*[45] were able to reduce the ICC misdiagnosis rate with CEUS LR-M from 38 to 12 cases by considering other criteria such as the presence of an intratumoral vein or an unclear boundary of the intratumoral non-enhanced area. However, we did not test these new criteria that require validation in multicentric and prospective studies. Another recent study by Huang *et al*[46] suggested that the integration of CEUS with the dosage of serum tumour markers (AFP and CA 19.9) improves the differentiation of LR-M nodules. Even though there are some limitations related to LR-M in this scenario, the adoption of this class of risk allows the improvement of diagnostic performance of CEUS for ICC, overcoming the drawbacks that resulted in the elimination of CEUS from the diagnostic flow charts of the most important hepatological international guidelines[3,8].

At present, CEUS LR-3 lesions are considered to hold an intermediate risk of malignancy, which is around 50% according to a recent study published by Terzi *et al*[22]. This rate was much lower in our case series (28.8%), which might be attributable to the lower figures of our study. Still, looking at the data from single centres in the multicentric study by Terzi *et al*[22], the rate of HCC in the CEUS LR-3 class ranged between 28.3% and 74.3%. One possible explanation for these results could be the high intrinsic heterogeneity of this class. Indeed, the algorithm only considers either the presence or absence of APHE, without any distinction between isoenhancement and hypoenhancement in all phases. However, in our clinical experience, hypo-hypo lesions are more likely to be malignant than iso-iso lesions. The present study confirmed this observation: Within the CEUS LR-3 class, the PPV for malignancy moved from 28.8% for CEUS LR-3 overall class to 2.6% for CEUS LR-3 iso-iso nodules, and 73.3% for CEUS LR-3 hypo-hypo nodules (Table 5). These considerations are in concordance with studies published before the advent of CEUS LI-RADS, when the problem of hypovascular nodules, which represent around 10% of HCC, was highlighted[47-49]. Likewise, we should be aware of the possibility of detecting ICC nodules in this class when a nodule shows hypoenhancement in all the phases; as observed in two out of 15 (13%) hypo-hypo nodules in our study. In light of these observations, we believe that it might be advantageous to split the CEUS LR-3 class into two subgroups (*e.g.*, CEUS LR-3a and CEUS LR-3b) in order to separate iso-iso lesions from other patterns. To the best of our knowledge, this is the first study suggesting a CEUS LR-3 refinement based on real-life results. We believe that more attention should be directed towards the behaviour of nodule enhancement, rather than focusing on the size of the lesion alone.

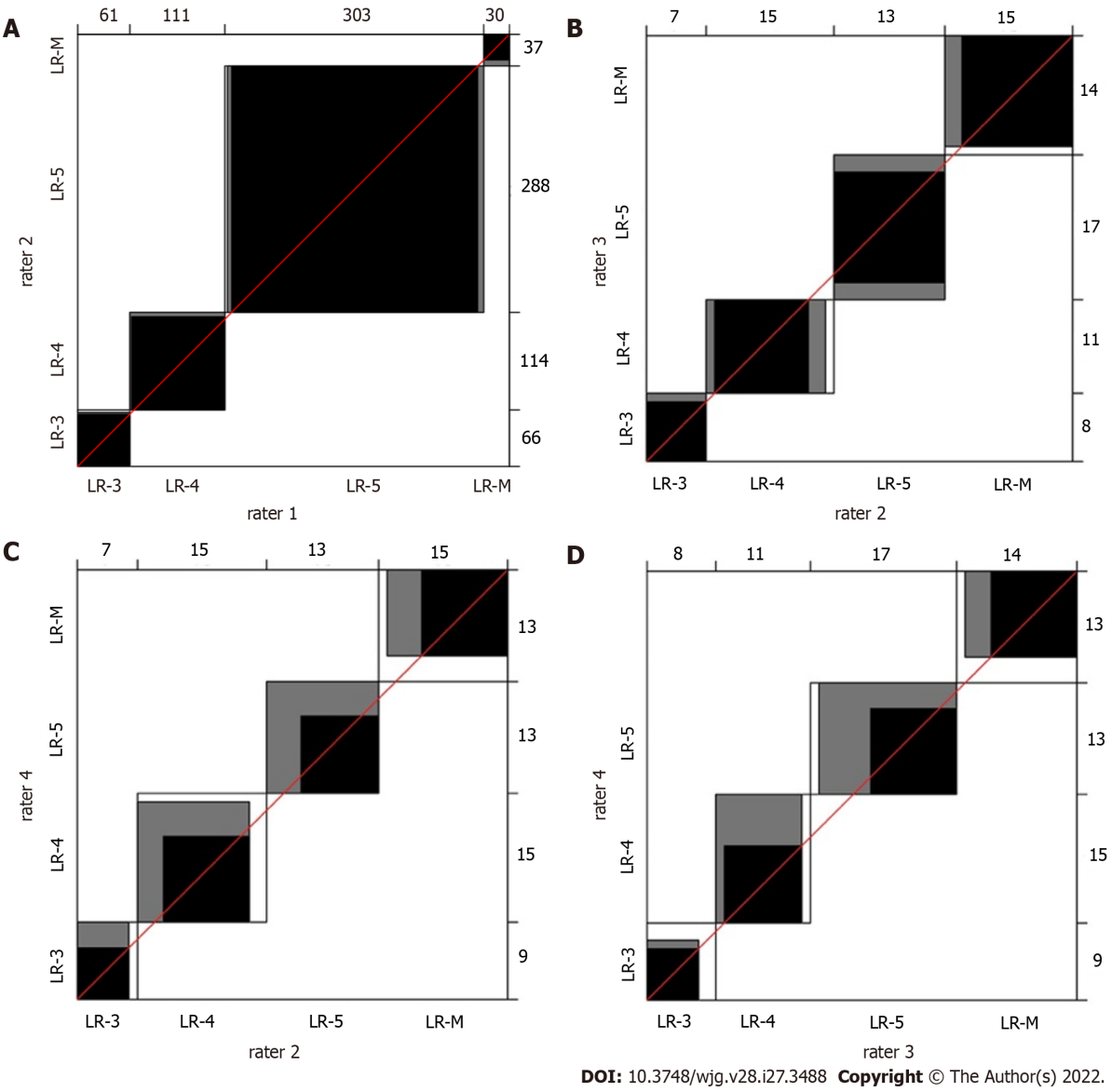

DOI: 10.3748/wjg.v28.i27.3488

Figure 4 Bangdiwala's agreement charts of the Contrast-enhanced ultrasound Liver Imaging Reporting and Data System class assignments between different raters. In the case of perfect agreement, the *k* rectangles are represented by perfect squares and the shaded squares determined by the diagonal cell entries are exactly equal to the rectangles; lesser agreement is visualized by comparing the area of the blackened squares to the area of the rectangles. A: Agreement chart between the two internal raters (1 and 2), with the exclusion of LR-1 and LR-2 classes due to their rarity (n = 505); B-D: Agreement charts among the three raters from different centres (2, 3, and 4) for the subgroup of 50 nodules. We list the agreement charts between raters 2 and 3 (B), between raters 2 and 4 (C), and between raters 3 and 4 (D).

Finally, this study demonstrated excellent inter-rater reliability of this classification system. Therefore, the use of CEUS LI-RADS in clinical practice could improve the reproducibility of CEUS and partially reduce the gap due to the difference in experience, as suggested by a recent study[50].

Our study also has some critical shortcomings, namely, its retrospective nature and the limited number of nodules analysed. These drawbacks are primarily due to the fact that data were collected from a single centre. Another debatable aspect of our investigation is the limited number of biopsies. However, we would like to highlight that current guidelines do not routinely recommend biopsy for nodules with typical HCC pattern on CT or MRI, allowing a non-invasive diagnosis[4,28].

Further prospective multicentric studies are warranted to confirm our findings and to investigate whether our considerations could be applied to the general population of patients with cirrhosis.

CONCLUSION

The present study supports the use of CEUS LI-RADS for the characterization of focal liver lesions in liver cirrhosis and the usefulness of LR-5 and LR-M classes to diagnose HCC and ICC, respectively. Additionally, our findings suggest that the merging of LR-4 and LR-5 classes provides innovative

benefits in terms of diagnostic accuracy for HCC. Furthermore, it seems reasonable to split the CEUS LR-3 class into two subgroups to differentiate the risk of malignancy between iso-iso nodules, which are more likely to be benign, and other patterns, namely, hypo-hypo nodules, which are more likely to be malignant and not specific for HCC.

ARTICLE HIGHLIGHTS

Research background

Patients affected by liver cirrhosis are at high risk of developing hepatocellular carcinoma (HCC) and other malignancies such us intrahepatic cholangiocellular carcinoma (ICC). Diagnostic tools to characterize new-onset nodules in cirrhosis include contrast-enhanced ultrasound (CEUS), but this technique has been challenged for the possibility of misdiagnosing HCC and ICC.

Research motivation

The CEUS Liver Imaging Reporting and Data System (CEUS LI-RADS) aims to refine CEUS interpretation in order to improve the differentiation of HCC from other malignancies. Nevertheless, its effectiveness in real-life context has not yet been well established.

Research objectives

To test the accuracy of CEUS LI-RADS in correctly diagnosing HCC and ICC in cirrhosis with LR-5 and LR-M class, respectively, to evaluate the performance of LR-4 and 5 merging class in the diagnosis of HCC, and to investigate the rate of malignancies in different LR-3 patterns.

Research methods

This study consecutively collected 511 nodules in 269 cirrhotic patients from December 2008 to January 2020. A CEUS LI-RADS class was retrospectively attributed to each nodule based on review of CEUS examination. Common diagnostic accuracy indexes were assessed for the following associations: CEUS LR-5 and HCC; CEUS LR-4 and 5 merged class and HCC; CEUS LR-M and ICC; CEUS LR-3 and malignancy. The diagnostic standard was either biopsy or computed tomography/magnetic resonance imaging. The frequency of malignant lesions in CEUS LR-3 subgroups with different CEUS patterns was also determined.

Research results

CEUS LR-5 showed a 97.7% specificity for HCC with a low sensitivity (67.6%), while the CEUS LR-4 and 5 merged class showed a 93.9% sensitivity and 94.3% specificity for HCC. CEUS LR-M predicted ICC with a 91.3% sensitivity and 96.7% specificity. CEUS LR-3 predominantly included benign lesions (28.8% of malignancies) but was heterogeneous as the hypo-hypo pattern showed a higher rate of malignant lesions (73.3%) than the iso-iso pattern (2.6%).

Research conclusions

HCC diagnosis could benefit from the merging of CEUS LI-RADS classes 4 and 5. In addition, splitting LR-3 class could be advantageous to differentiate iso-iso nodules from other patterns with a higher risk of malignancy.

Research perspectives

Further prospective multicentric studies are necessary to confirm and extend our findings to the general population.

ACKNOWLEDGEMENTS

The authors thank Cabigiosu F for his help in data entry, and Fois SS for contributing to English language revision of the manuscript.

FOOTNOTES

Author contributions: Vidili G designed the study, performed contrast-enhanced ultrasound examinations, biopsies, and the blinded review of cases, and wrote and revised the manuscript; Arru M performed the blinded review of the cases, collected and analysed the data, and participated in paper writing and review; Solinas G performed the statistical analysis and participated in the final draft; Calvisi DF collected and analysed the data, and participated in writing, review, and editing of the manuscript; Meloni P, Sauchella A, and Di Lembo E participated in collecting and

preparing the data for the analysis; Turilli D and Fabio C performed computed tomography and magnetic resonance imaging scans and participated in data collection; Cossu A reviewed the pathology material; Madeddu G participated in data collection and writing the paper; Zocco MA and Iannetti G performed the external blinded review of the cases; Delitala AP and Babudieri S participated in data analysis and writing of the manuscript; Manetti R participated in writing and reviewing the final draft; all authors have read and agreed to the final version of the manuscript.

Supported by the Fondazione di Sardegna, No. FDS2019VIDILI; and the University of Sassari, No. FAR2019.

Institutional review board statement: This study was reviewed and approved by the Ethics Committee of Azienda Ospedaliero Universitaria di Sassari and the Ethics Committee of Azienda Ospedaliero Universitaria di Cagliari (No. PG/2020/16814).

Informed consent statement: All study participants, or their legal guardian, provided informed written consent prior to study enrollment.

Conflict-of-interest statement: There are no conflicts of interest to report.

Data sharing statement: Data presented in this study is available on request from the corresponding author.

Country/Territory of origin: Italy

ORCID number: Gianpaolo Vidili 0000-0003-0003-1272; Marco Arru 0000-0002-7112-5025; Giuliana Solinas 0000-0003-2174-0983; Diego Francesco Calvisi 0000-0002-6038-8567; Pierluigi Meloni 0000-0003-3313-0445; Assunta Sauchella 0000-0003-1116-7458; Davide Turilli 0000-0002-2063-994X; Claudio Fabio 0000-0002-5372-1552; Antonio Cossu 0000-0002-2390-2205; Giordano Madeddu 0000-0001-6099-2273; Sergio Babudieri 0000-0001-7291-8687; Maria Assunta Zocco 0000-0002-0814-9542; Giovanni Iannetti 0000-0002-1880-0829; Enza Di Lembo 0000-0003-1652-600X; Alessandro Palmerio Delitala 0000-0003-1729-8969; Roberto Manetti 0000-0001-7376-2303.

S-Editor: Chen YL
L-Editor: Wang TQ
P-Editor: Wu RR

REFERENCES

1 **Sung H**, Ferlay J, Siegel RL, Laversanne M, Soerjomataram I, Jemal A, Bray F. Global Cancer Statistics 2020: GLOBOCAN Estimates of Incidence and Mortality Worldwide for 36 Cancers in 185 Countries. *CA Cancer J Clin* 2021; **71**: 209-249 [PMID: 33538338 DOI: 10.3322/caac.21660]

2 **Italian Association for the Study of the Liver (AISF)**, AISF Expert Panel; AISF Coordinating Committee, Bolondi L, Cillo U, Colombo M, Craxì A, Farinati F, Giannini EG, Golfieri R, Levrero M, Pinna AD, Piscaglia F, Raimondo G, Trevisani F, Bruno R, Caraceni P, Ciancio A, Coco B, Fraquelli M, Rendina M, Squadrito G, Toniutto P. Position paper of the Italian Association for the Study of the Liver (AISF): the multidisciplinary clinical approach to hepatocellular carcinoma. *Dig Liver Dis* 2013; **45**: 712-723 [PMID: 23769756 DOI: 10.1016/j.dld.2013.01.012]

3 **European Association For The Study Of The Liver**. EASL-EORTC clinical practice guidelines: management of hepatocellular carcinoma. *J Hepatol* 2012; **56**: 908-943 [DOI: 10.1016/j.jhep.2012.03.006]

4 **European Association for the Study of the Liver**. EASL Clinical Practice Guidelines: Management of hepatocellular carcinoma. *J Hepatol* 2018; **69**: 182-236 [DOI: 10.1016/j.jhep.2018.03.019]

5 **Bolondi L**, Sofia S, Siringo S, Gaiani S, Casali A, Zironi G, Piscaglia F, Gramantieri L, Zanetti M, Sherman M. Surveillance programme of cirrhotic patients for early diagnosis and treatment of hepatocellular carcinoma: a cost effectiveness analysis. *Gut* 2001; **48**: 251-259 [PMID: 11156649 DOI: 10.1136/gut.48.2.251]

6 **Vidili G**, De Sio I, D'Onofrio M, Mirk P, Bertolotto M, Schiavone C; SIUMB experts committee. SIUMB guidelines and recommendations for the correct use of ultrasound in the management of patients with focal liver disease. *J Ultrasound* 2019; **22**: 41-51 [PMID: 30580390 DOI: 10.1007/s40477-018-0343-0]

7 **Claudon M**, Dietrich CF, Choi BI, Cosgrove DO, Kudo M, Nolsøe CP, Piscaglia F, Wilson SR, Barr RG, Chammas MC, Chaubal NG, Chen MH, Clevert DA, Correas JM, Ding H, Forsberg F, Fowlkes JB, Gibson RN, Goldberg BB, Lassau N, Leen EL, Mattrey RF, Moriyasu F, Solbiati L, Weskott HP, Xu HX; World Federation for Ultrasound in Medicine; European Federation of Societies for Ultrasound. Guidelines and good clinical practice recommendations for Contrast Enhanced Ultrasound (CEUS) in the liver - update 2012: A WFUMB-EFSUMB initiative in cooperation with representatives of AFSUMB, AIUM, ASUM, FLAUS and ICUS. *Ultrasound Med Biol* 2013; **39**: 187-210 [PMID: 23137926 DOI: 10.1016/j.ultrasmedbio.2012.09.002]

8 **Vilana R**, Forner A, Bianchi L, García-Criado A, Rimola J, de Lope CR, Reig M, Ayuso C, Brú C, Bruix J. Intrahepatic

peripheral cholangiocarcinoma in cirrhosis patients may display a vascular pattern similar to hepatocellular carcinoma on contrast-enhanced ultrasound. *Hepatology* 2010; **51**: 2020-2029 [PMID: 20512990 DOI: 10.1002/hep.23600]

9 **de Sio I**, Iadevaia MD, Vitale LM, Niosi M, Del Prete A, de Sio C, Romano L, Funaro A, Meucci R, Federico A, Loguercio C, Romano M. Optimized contrast-enhanced ultrasonography for characterization of focal liver lesions in cirrhosis: A single-center retrospective study. *United European Gastroenterol J* 2014; **2**: 279-287 [PMID: 25083285 DOI: 10.1177/2050640614538964]

10 **Forner A**, Vidili G, Rengo M, Bujanda L, Ponz-Sarvisé M, Lamarca A. Clinical presentation, diagnosis and staging of cholangiocarcinoma. *Liver Int* 2019; **39** Suppl 1: 98-107 [PMID: 30831002 DOI: 10.1111/liv.14086]

11 **Wildner D**, Schellhaas B, Strack D, Goertz RS, Pfeifer L, Fiessler C, Neurath MF, Strobel D. Differentiation of malignant liver tumors by software-based perfusion quantification with dynamic contrast-enhanced ultrasound (DCEUS). *Clin Hemorheol Microcirc* 2019; **71**: 39-51 [PMID: 29865043 DOI: 10.3233/CH-180378]

12 **Liu GJ**, Wang W, Lu MD, Xie XY, Xu HX, Xu ZF, Chen LD, Wang Z, Liang JY, Huang Y, Li W, Liu JY. Contrast-Enhanced Ultrasound for the Characterization of Hepatocellular Carcinoma and Intrahepatic Cholangiocarcinoma. *Liver Cancer* 2015; **4**: 241-252 [PMID: 26779444 DOI: 10.1159/000367738]

13 **Galassi M**, Iavarone M, Rossi S, Bota S, Vavassori S, Rosa L, Leoni S, Venerandi L, Marinelli S, Sangiovanni A, Veronese L, Fraquelli M, Granito A, Golfieri R, Colombo M, Bolondi L, Piscaglia F. Patterns of appearance and risk of misdiagnosis of intrahepatic cholangiocarcinoma in cirrhosis at contrast enhanced ultrasound. *Liver Int* 2013; **33**: 771-779 [PMID: 23445369 DOI: 10.1111/liv.12124]

14 **Chen LD**, Ruan SM, Liang JY, Yang Z, Shen SL, Huang Y, Li W, Wang Z, Xie XY, Lu MD, Kuang M, Wang W. Differentiation of intrahepatic cholangiocarcinoma from hepatocellular carcinoma in high-risk patients: A predictive model using contrast-enhanced ultrasound. *World J Gastroenterol* 2018; **24**: 3786-3798 [PMID: 30197484 DOI: 10.3748/wjg.v24.i33.3786]

15 **American College of Radiology**. CEUS LI RADS v2017 CORE. 2017. Avaiable from: https://www.acr.org/Quality-Safety/Resources/LIRADS

16 **Wilson SR**, Lyshchik A, Piscaglia F, Cosgrove D, Jang HJ, Sirlin C, Dietrich CF, Kim TK, Willmann JK, Kono Y. CEUS LI-RADS: algorithm, implementation, and key differences from CT/MRI. *Abdom Radiol (NY)* 2018; **43**: 127-142 [PMID: 28819825 DOI: 10.1007/s00261-017-1250-0]

17 **Lyshchik A**, Kono Y, Dietrich CF, Jang HJ, Kim TK, Piscaglia F, Vezeridis A, Willmann JK, Wilson SR. Contrast-enhanced ultrasound of the liver: technical and lexicon recommendations from the ACR CEUS LI-RADS working group. *Abdom Radiol (NY)* 2018; **43**: 861-879 [PMID: 29151131 DOI: 10.1007/s00261-017-1392-0]

18 **Kim TK**, Noh SY, Wilson SR, Kono Y, Piscaglia F, Jang HJ, Lyshchik A, Dietrich CF, Willmann JK, Vezeridis A, Sirlin CB. Contrast-enhanced ultrasound (CEUS) liver imaging reporting and data system (LI-RADS) 2017 - a review of important differences compared to the CT/MRI system. *Clin Mol Hepatol* 2017; **23**: 280-289 [PMID: 28911220 DOI: 10.3350/cmh.2017.0037]

19 **Rimola J**, Forner A, Tremosini S, Reig M, Vilana R, Bianchi L, Rodríguez-Lope C, Solé M, Ayuso C, Bruix J. Non-invasive diagnosis of hepatocellular carcinoma ≤ 2 cm in cirrhosis. Diagnostic accuracy assessing fat, capsule and signal intensity at dynamic MRI. *J Hepatol* 2012; **56**: 1317-1323 [PMID: 22314420 DOI: 10.1016/j.jhep.2012.01.004]

20 **Barreiros AP**, Piscaglia F, Dietrich CF. Contrast enhanced ultrasound for the diagnosis of hepatocellular carcinoma (HCC): comments on AASLD guidelines. *J Hepatol* 2012; **57**: 930-932 [PMID: 22739095 DOI: 10.1016/j.jhep.2012.04.018]

21 **Huang JY**, Li JW, Lu Q, Luo Y, Lin L, Shi YJ, Li T, Liu JB, Lyshchik A. Diagnostic Accuracy of CEUS LI-RADS for the Characterization of Liver Nodules 20 mm or Smaller in Patients at Risk for Hepatocellular Carcinoma. *Radiology* 2020; **294**: 329-339 [PMID: 31793849 DOI: 10.1148/radiol.2019191086]

22 **Terzi E**, Iavarone M, Pompili M, Veronese L, Cabibbo G, Fraquelli M, Riccardi L, De Bonis L, Sangiovanni A, Leoni S, Zocco MA, Rossi S, Alessi N, Wilson SR, Piscaglia F; CEUS LI-RADS Italy study group collaborators:. Contrast ultrasound LI-RADS LR-5 identifies hepatocellular carcinoma in cirrhosis in a multicenter restropective study of 1,006 nodules. *J Hepatol* 2018; **68**: 485-492 [PMID: 29133247 DOI: 10.1016/j.jhep.2017.11.007]

23 **Huang Z**, Zhou P, Li S, Li K. MR versus CEUS LI-RADS for Distinguishing Hepatocellular Carcinoma from other Hepatic Malignancies in High-Risk Patients. Ultrasound Med Biol 2021; 47: 1244-1252 [PMID: 33610338 DOI: 10.1016/j.ultrasmedbio.2021.01.020]

24 **Li S**, Zhou L, Chen R, Chen Y, Niu Z, Qian L, Fang Y, Xu L, Xu H, Zhang L. Diagnostic efficacy of contrast-enhanced ultrasound versus MRI Liver Imaging Reporting and Data System (LI-RADS) for categorising hepatic observations in patients at risk of hepatocellular carcinoma. Clin Radiol 2021; 76: 161.e1-161.e10 [PMID: 33198943 DOI: 10.1016/j.crad.2020.10.009]

25 **Makoyeva A**, Kim TK, Jang HJ, Medellin A, Wilson SR. Use of CEUS LI-RADS for the Accurate Diagnosis of Nodules in Patients at Risk for Hepatocellular Carcinoma: A Validation Study. *Radiol Imaging Cancer* 2020; **2**: e190014 [PMID: 33778701 DOI: 10.1148/rycan.2020190014]

26 **Pan JM**, Chen W, Zheng YL, Cheng MQ, Zeng D, Huang H, Huang Y, Xie XY, Lu MD, Kuang M, Hu HT, Chen LD, Wang W. Tumor size-based validation of contrast-enhanced ultrasound liver imaging reporting and data system (CEUS LI-RADS) 2017 for hepatocellular carcinoma characterizing. *Br J Radiol* 2021; **94**: 20201359 [PMID: 34545763 DOI: 10.1259/bjr.20201359]

27 **Lv K**, Cao X, Dong Y, Geng D, Zhang J. CT/MRI LI-RADS version 2018 versus CEUS LI-RADS version 2017 in the diagnosis of primary hepatic nodules in patients with high-risk hepatocellular carcinoma. Ann Transl Med 2021; 9: 1076 [PMID: 34422988 DOI: 10.21037/atm-21-1035]

28 **Bruix J**, Sherman M; American Association for the Study of Liver Diseases. Management of hepatocellular carcinoma: an update. *Hepatology* 2011; **53**: 1020-1022 [PMID: 21374666 DOI: 10.1002/hep.24199]

29 **Bangdiwala SI**, Shankar V. The agreement chart. *BMC Med Res Methodol* 2013; **13**: 97 [PMID: 23890315 DOI: 10.1186/1471-2288-13-97]

30 **Landis JR**, Koch GG. The measurement of observer agreement for categorical data. *Biometrics* 1977; **33**: 159-174 [PMID:

843571]
31 **Schellhaas B**, Bernatik T, Bohle W, Borowitzka F, Chang J, Dietrich CF, Dirks K, Donoval R, Drube K, Friedrich-Rust M, Gall C, Gittinger F, Gutermann M, Haenle MM, von Herbay A, Ho CH, Hochdoerffer R, Hoffmann T, Hüttig M, Janson C, Jung EM, Jung N, Karlas T, Klinger C, Kornmehl A, Kratzer W, Krug S, Kunze G, Leitlein J, Link A, Lottspeich C, Marano A, Mauch M, Moleda L, Neesse A, Petzold G, Potthoff A, Praktiknjo M, Rösner KD, Schanz S, Schultheiß M, Sivanathan V, Stock J, Thomsen T, Vogelpohl J, Vogt C, Wagner S, Wiegard C, Wiesinger I, Will U, Ziesch M, Zimmermann P, Strobel D. Contrast-Enhanced Ultrasound Algorithms (CEUS-LIRADS/ESCULAP) for the Noninvasive Diagnosis of Hepatocellular Carcinoma - A Prospective Multicenter DEGUM Study. *Ultraschall Med* 2021; **42**: e20 [PMID: 32717752 DOI: 10.1055/a-1220-8561]
32 **Peng J**, Zhang T, Wang H, Ma X. The Value of Contrast-Enhanced Ultrasound Liver Imaging Reporting and Data System in the Diagnosis of Hepatocellular Carcinoma: A Meta-Analysis. *J Ultrasound Med* 2022; **41**: 1537-1547 [PMID: 34617296 DOI: 10.1002/jum.15837]
33 **Giorgio A**, Montesarchio L, Gatti P, Amendola F, Matteucci P, Santoro B, Merola MG, Merola F, Coppola C, Giorgio V. Contrast-Enhanced Ultrasound: a Simple and Effective Tool in Defining a Rapid Diagnostic Work-up for Small Nodules Detected in Cirrhotic Patients during Surveillance. *J Gastrointestin Liver Dis* 2016; **25**: 205-211 [PMID: 27308652 DOI: 10.15403/jgld.2014.1121.252.chu]
34 **Leoni S**, Piscaglia F, Granito A, Borghi A, Galassi M, Marinelli S, Terzi E, Bolondi L. Characterization of primary and recurrent nodules in liver cirrhosis using contrast-enhanced ultrasound: which vascular criteria should be adopted? *Ultraschall Med* 2013; **34**: 280-287 [PMID: 23616066 DOI: 10.1055/s-0033-1335024]
35 **Baron RL**, Oliver JH 3rd, Dodd GD 3rd, Nalesnik M, Holbert BL, Carr B. Hepatocellular carcinoma: evaluation with biphasic, contrast-enhanced, helical CT. *Radiology* 1996; **199**: 505-511 [PMID: 8668803 DOI: 10.1148/radiology.199.2.8668803]
36 **Oliver JH 3rd**, Baron RL, Federle MP, Rockette HE Jr. Detecting hepatocellular carcinoma: value of unenhanced or arterial phase CT imaging or both used in conjunction with conventional portal venous phase contrast-enhanced CT imaging. *AJR Am J Roentgenol* 1996; **167**: 71-77 [PMID: 8659425 DOI: 10.2214/ajr.167.1.8659425]
37 **Hwang GJ**, Kim MJ, Yoo HS, Lee JT. Nodular hepatocellular carcinomas: detection with arterial-, portal-, and delayed-phase images at spiral CT. *Radiology* 1997; **202**: 383-388 [PMID: 9015062 DOI: 10.1148/radiology.202.2.9015062]
38 **Schellhaas B**, Görtz RS, Pfeifer L, Kielisch C, Neurath MF, Strobel D. Diagnostic accuracy of contrast-enhanced ultrasound for the differential diagnosis of hepatocellular carcinoma: ESCULAP versus CEUS-LI-RADS. *Eur J Gastroenterol Hepatol* 2017; **29**: 1036-1044 [PMID: 28562394 DOI: 10.1097/MEG.0000000000000916]
39 **Li J**, Ling W, Chen S, Ma L, Yang L, Lu Q, Luo Y. The interreader agreement and validation of contrast-enhanced ultrasound liver imaging reporting and data system. *Eur J Radiol* 2019; **120**: 108685 [PMID: 31606712 DOI: 10.1016/j.ejrad.2019.108685]
40 **Schellhaas B**, Pfeifer L, Kielisch C, Goertz RS, Neurath MF, Strobel D. Interobserver Agreement for Contrast-Enhanced Ultrasound (CEUS)-Based Standardized Algorithms for the Diagnosis of Hepatocellular Carcinoma in High-Risk Patients. *Ultraschall Med* 2018; **39**: 667-674 [PMID: 29879746 DOI: 10.1055/a-0612-7887]
41 **Yang J**, Zhang YH, Li JW, Shi YY, Huang JY, Luo Y, Liu JB, Lu Q. Contrast-enhanced ultrasound in association with serum biomarkers for differentiating combined hepatocellular-cholangiocarcinoma from hepatocellular carcinoma and intrahepatic cholangiocarcinoma. *World J Gastroenterol* 2020; **26**: 7325-7337 [PMID: 33362387 DOI: 10.3748/wjg.v26.i46.7325]
42 **Li F**, Li Q, Liu Y, Han J, Zheng W, Huang Y, Zheng X, Cao L, Zhou JH. Distinguishing intrahepatic cholangiocarcinoma from hepatocellular carcinoma in patients with and without risks: the evaluation of the LR-M criteria of contrast-enhanced ultrasound liver imaging reporting and data system version 2017. *Eur Radiol* 2020; **30**: 461-470 [PMID: 31297632 DOI: 10.1007/s00330-019-06317-2]
43 **Ding J**, Qin Z, Zhou Y, Zhou H, Zhang Q, Wang Y, Jing X, Wang F. Impact of Revision of the LR-M Criteria on the Diagnostic Performance of Contrast-Enhanced Ultrasound LI-RADS. *Ultrasound Med Biol* 2021; **47**: 3403-3410 [PMID: 34598799 DOI: 10.1016/j.ultrasmedbio.2021.08.007]
44 **Zeng D**, Xu M, Liang JY, Cheng MQ, Huang H, Pan JM, Huang Y, Tong WJ, Xie XY, Lu MD, Kuang M, Chen LD, Hu HT, Wang W. Using new criteria to improve the differentiation between HCC and non-HCC malignancies: clinical practice and discussion in CEUS LI-RADS 2017. *Radiol Med* 2022; **127**: 1-10 [PMID: 34665430 DOI: 10.1007/s11547-021-01417-w]
45 **Chen LD**, Ruan SM, Lin Y, Liang JY, Shen SL, Hu HT, Huang Y, Li W, Wang Z, Xie XY, Lu MD, Kuang M, Wang W. Comparison between M-score and LR-M in the reporting system of contrast-enhanced ultrasound LI-RADS. *Eur Radiol* 2019; **29**: 4249-4257 [PMID: 30569182 DOI: 10.1007/s00330-018-5927-8]
46 **Huang JY**, Li JW, Ling WW, Li T, Luo Y, Liu JB, Lu Q. Can contrast enhanced ultrasound differentiate intrahepatic cholangiocarcinoma from hepatocellular carcinoma? *World J Gastroenterol* 2020; **26**: 3938-3951 [PMID: 32774068 DOI: 10.3748/wjg.v26.i27.3938]
47 **Boozari B**, Soudah B, Rifai K, Schneidewind S, Vogel A, Hecker H, Hahn A, Schlue J, Dietrich CF, Bahr MJ, Kubicka S, Manns MP, Gebel M. Grading of hypervascular hepatocellular carcinoma using late phase of contrast enhanced sonography - a prospective study. *Dig Liver Dis* 2011; **43**: 484-490 [PMID: 21377941 DOI: 10.1016/j.dld.2011.01.001]
48 **Choi BI**, Lee JM, Kim TK, Dioguardi Burgio M, Vilgrain V. Diagnosing Borderline Hepatic Nodules in Hepatocarcinogenesis: Imaging Performance. *AJR Am J Roentgenol* 2015; **205**: 10-21 [PMID: 26102378 DOI: 10.2214/AJR.14.12655]
49 **Bolondi L**, Gaiani S, Celli N, Golfieri R, Grigioni WF, Leoni S, Venturi AM, Piscaglia F. Characterization of small nodules in cirrhosis by assessment of vascularity: the problem of hypovascular hepatocellular carcinoma. *Hepatology* 2005; **42**: 27-34 [PMID: 15954118 DOI: 10.1002/hep.20728]
50 **Li W**, Li L, Zhuang BW, Ruan SM, Hu HT, Huang Y, Lin MX, Xie XY, Kuang M, Lu MD, Chen LD, Wang W. Inter-reader agreement of CEUS LI-RADS among radiologists with different levels of experience. *Eur Radiol* 2021; **31**: 6758-6767 [PMID: 33675388 DOI: 10.1007/s00330-021-07777-1]

Published by **Baishideng Publishing Group Inc**
7041 Koll Center Parkway, Suite 160, Pleasanton, CA 94566, USA
Telephone: +1-925-3991568
E-mail: bpgoffice@wjgnet.com
Help Desk: https://www.f6publishing.com/helpdesk
https://www.wjgnet.com